



Dimorphism and magnetic properties in iron rare earth germanates

C. Cascales^{a,*}, L. Bucio^{1,a}, E. Gutiérrez Puebla^a, I. Rasines^a, M.T. Fernández Díaz^b

^aInstituto de Ciencia de Materiales de Madrid, CSIC. Cantoblanco, E-28049 Madrid, Spain

^bInstitut Laue-Langevin, 156X, F-38042 Grenoble Cedex, France

Abstract

Polycrystalline samples of iron and lanthanide FeRGe_2O_7 germanates, $\text{R}=\text{Dy, Ho, Er, Yb}$ have been prepared. They present the new II- FeRGe_2O_7 structure type, S.G. $\text{P2}_1/\text{m}$ (No. 11) $Z=4$. Results of the refinements from neutron diffraction data for Dy and Yb compounds as well as X-ray data (Ho, Er) are given. Lattice dimensions are $a/\text{Å}=9.6391(4), 9.635(1), 9.646(2)$ and $9.6554(5)$; $b/\text{Å}=8.4743(3), 8.475(1), 8.511(1)$ and $8.5125(4)$; $c/\text{Å}=6.7113(3), 6.6701(9), 6.655(1)$ and $6.6804(4)$; and $\beta/^\circ=100.538(7), 100.612(7), 100.83(1)$ and $100.733(3)$, for $\text{R}=\text{Dy, Ho, Er}$ and Yb , respectively. Magnetic susceptibility measurements between 350 and 1.7 K reveal the existence of two separated anomalies for each of the four compounds, which appear at T_1 and T_2 ($T_2 < T_1$): 41 and 24 K, 38 and 17 K, 40 and 8 K, 38 and 4 K, respectively. T_1 coincides with the setting up of magnetic ordering in Fe^{3+} and R^{3+} sublattices, as determined by neutron diffraction in Tb and Dy compounds, and correspond to the Néel temperatures. $\chi(T)$ maxima at T_2 do not correspond to any phase transition but they are caused by the exchange interaction of R^{3+} magnetic moments with the ordered iron subsystem. The crystal structure and magnetic properties of these FeRGe_2O_7 compounds are compared with those of I- FeRGe_2O_7 ($\text{R}=\text{Pr, Nd}$ and Gd) and other II- ($\text{R}=\text{Y, Tb}$) compounds. © 1998 Elsevier Science S.A.

Keywords: Rare earth germanates; Crystal structures; Magnetic structure; Magnetic properties

1. Introduction

FeRGe_2O_7 germanates ($\text{R}=\text{Y, La}$, and lanthanides) have received considerable attention because of the interesting magnetic properties associated to their structural characteristics. The phase formation along this series has been found to be dependent on the size of R, with two different monoclinic crystal structures: I, $\text{NdAlGe}_2\text{O}_7$ type, [1–3], S.G. $\text{P2}_1/\text{c}$ (No. 14), $Z=4$, for the larger rare earths, La to Gd; and II, a novel structure type, FeYGe_2O_7 , S.G. $\text{P2}_1/\text{m}$ (No. 11), $Z=4$, recently determined [4] *ab initio*, for the smaller ones, Y, Tb–Yb.

Since I- and II- FeRGe_2O_7 have different crystal structures, qualitative differences in the magnetic properties of the two groups may be expected. It is known [2,3] that germanates of the first type are antiferromagnetic at very low temperatures, whereas the lack of knowledge on the crystal structure of II- FeRGe_2O_7 did not allow until recently [4] to decide between the two alternative proposed models [5] to explain the observed magnetic properties.

This paper presents the crystal structure refinement from neutron diffraction data for $\text{R}=\text{Dy}$ and Yb , the structural characterisation of $\text{R}=\text{Ho}$ and Er from X-ray powder diffraction data, and the results of magnetization measurements for the four compounds between 350 and 1.7 K, which are compared with those for some other germanates with the same stoichiometry.

2. Experimental

Polycrystalline samples of FeRGe_2O_7 , $\text{R}=\text{Dy, Ho, Er}$ and Yb , were prepared by solid state reaction in a similar way to the previously described [4]. X-ray powder diffraction (XRPD) data were recorded at room temperature using a SIEMENS Kristalloflex 810 generator, graphite monochromated $\text{CuK}\alpha$ radiation, and a computer-controlled D-500 goniometer. Neutron powder diffraction (NPD) patterns for the Dy and Yb compounds were collected on the D2B (room temperature) and D1B (1.7 to 60 K) powder diffractometers at the Institut Laue-Langevin of Grenoble, using wavelengths of 1.595 and 2.52 Å, respectively. Further details can be found elsewhere [4]. A SQUID magnetometer (Quantum Design)

*Corresponding author.

¹Permanent address: Departamento de Estado Sólido. Instituto de Física, UNAM, Apdo. postal 20-364, 01000 Mexico DF, Mexico.

operating from 350 to 1.7 K at 5000 to 1000 Oe was used to perform the magnetic measurements. Diamagnetic corrections [6] for the magnetic susceptibilities were considered.

3. Crystal structure

Table 1 includes diffraction data for FeRGe_2O_7 , R=Dy, Ho, Er and Yb. Those for R=Y, Tb [4] have been added for comparison. The results of the profile Rietveld refinement from NPD data, positional and thermal parameters, for the Dy compound, are given in Table 2. In Fig. 1. the neutron diffraction pattern for the same compound at room temperature is shown.

In these germanates there are three kinds of coordination polyhedra: FeO_6 distorted octahedra joined in pairs by edge sharing; capped RO_7 octahedra, with all the R–O distances being of different lengths; and four kind of GeO_4 tetrahedra associated by corner-sharing to form Ge_2O_7 diorthogroups.

RO_7 polyhedra are connected alternately by either a vertex or an edge into chains along the b axis, Fig. 2. In the same direction only isolated pairs of FeO_6 octahedra exist, as can be seen also in Fig. 2. Flattened chains of RO_7 polyhedra are linked in the c direction through pairs of FeO_6 octahedra with which they share edges forming layers running parallel to the bc crystal plane. Although Ge_2O_7 diorthogroups are not connected neither in a nor in b directions, they play a bridging role between parallel RO_7 - and FeO_6 -containing sheets, as shown by Fig. 3. Only one of these four types of tetrahedra, $\text{Ge}(2)\text{O}_4$, shares an edge with a RO_7 polyhedron, whereas the remaining GeO_4 are joined only by common corners to adjacent bc layers.

In the I- FeRGe_2O_7 structural type [1–3], chains of edge-sharing flexed RO_9 tricapped trigonal prisms are lying along the a axis, going linked alternately through an edge or a corner from isolated FeO_5 distorted trigonal bipyramids in the c direction. Thus, although they have the same stoichiometry, I- and II- FeRGe_2O_7 present important differences when their coordination polyhedra, especially

Table 2

Final refined positional and thermal parameters for $\text{DyFeGe}_2\text{O}_7$ from NPD (D2B) at room temperature.

		x/a	y/b	z/c	$B(\text{\AA}^2)$
Dy	(4f)	0.7450(19)	0.5377(6)	0.7490(24)	0.76(18)
Ge1	(2e)	0.4796(38)	0.25	0.9529(54)	0.49(21)
Ge2	(2e)	0.5482(30)	0.25	0.4611(40)	0.49(21)
Ge3	(2e)	0.9496(31)	0.25	0.0024(39)	0.49(21)
Ge4	(2e)	0.0318(36)	0.25	0.5586(58)	0.49(21)
Fe	(4f)	0.7524(31)	0.4488(11)	0.2417(52)	0.50(30)
O1	(4f)	0.6462(37)	0.4250(43)	0.4791(41)	0.29(17)
O2	(2e)	0.8830(51)	0.25	0.3602(76)	0.29(17)
O3	(2e)	0.9459(35)	0.25	0.7287(44)	0.29(17)
O4	(2e)	0.5732(36)	0.25	0.7134(51)	0.29(17)
O5	(4f)	0.8690(35)	0.0789(43)	0.0381(40)	0.29(17)
O6	(4e)	0.1116(47)	0.25	0.1322(64)	0.29(17)
O7	(4f)	0.1529(27)	0.0957(34)	0.5500(43)	0.29(17)
O8	(2e)	0.3770(46)	0.25	0.3397(63)	0.29(17)
O9	(2e)	0.6315(49)	0.25	0.1516(62)	0.29(17)
O10	(4f)	0.6263(27)	0.5782(35)	0.0368(44)	0.29(17)

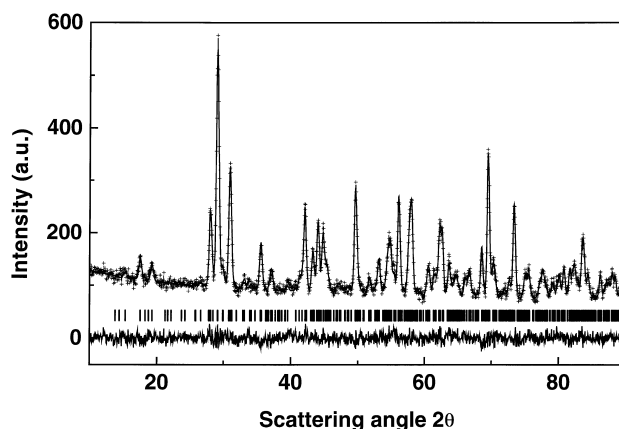


Fig. 1. Neutron diffraction pattern of $\text{DyFeGe}_2\text{O}_7$ (D2B-ILL) at room temperature. The solid line is the calculated profile and vertical marks correspond to the position of the Bragg reflections for the crystallographic structure. The difference curve is plotted at the bottom of the figure.

those of the rare earth and iron cations, and connectivities between all of them are compared. This can be clearly observed opposing Fig. 4a and b corresponding to I- FeRGe_2O_7 , to the previous Fig. 2 and Fig. 3 for II- FeRGe_2O_7 .

Table 1

Lattice parameters for FeRGe_2O_7 , R=Y, Tb, Dy, Ho, Er and Yb, S.G. $P2_1/m$, Z=4

	Y ^{a,c}	Tb ^{b,c}	Dy ^b	Ho ^a	Er ^a	Yb ^b
a (Å)	9.6552 (4)	9.6377 (3)	9.6391 (4)	9.635 (1)	9.646 (2)	9.6554 (5)
b (Å)	8.5197 (3)	8.4794 (2)	8.4743 (3)	8.475 (1)	8.511 (1)	8.5125 (4)
c (Å)	6.6746 (3)	6.7383 (2)	6.7113 (3)	6.6701 (9)	6.655 (1)	6.6804 (3)
β (°)	100.761 (2)	100.381 (2)	100.538 (1)	100.612 (7)	100.83 (1)	100.733 (3)
R_p	8.51	3.57	4.84	7.51	8.91	5.50
R_{exp}	9.81	2.42	6.08	7.02	7.62	2.18
χ^2	1.29	3.60	1.02	1.85	2.91	1.80
R_{Bragg}	6.64	5.90	5.23	9.16	9.33	9.91
R_f	5.79	3.39	3.80	5.39	5.95	6.24

^a From XRPD data; ^b from D2B NPD data; ^c data for R=Y and Tb are from [4].

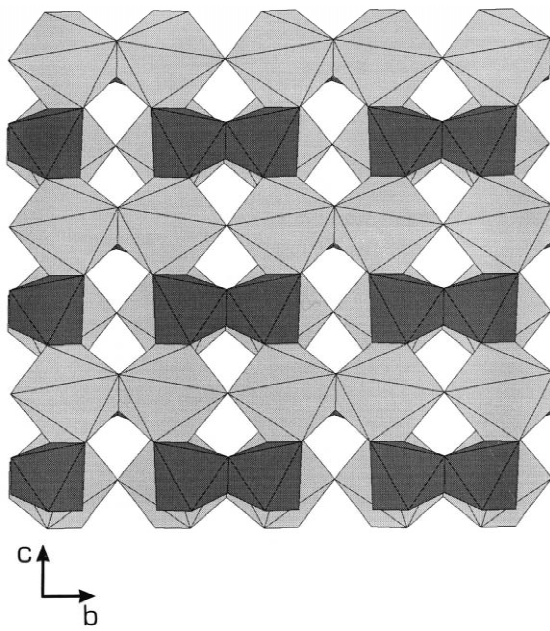


Fig. 2. Projection of the crystal structure of $\text{DyFeGe}_2\text{O}_7$ on the bc plane, depicting the DyO_7 chains along the b axis linked in the c direction through the pairs of FeO_6 .

4. Magnetic measurements

The evolution of the magnetic susceptibility χ between ~ 50 and 350 K follows a Curie–Weiss law for all $\text{II-FeRGe}_2\text{O}_7$ compounds. However, at lower temperatures $\chi(T)$ curves present peaks that indicate transitions to antiferromagnetically ordered states. With the exception of

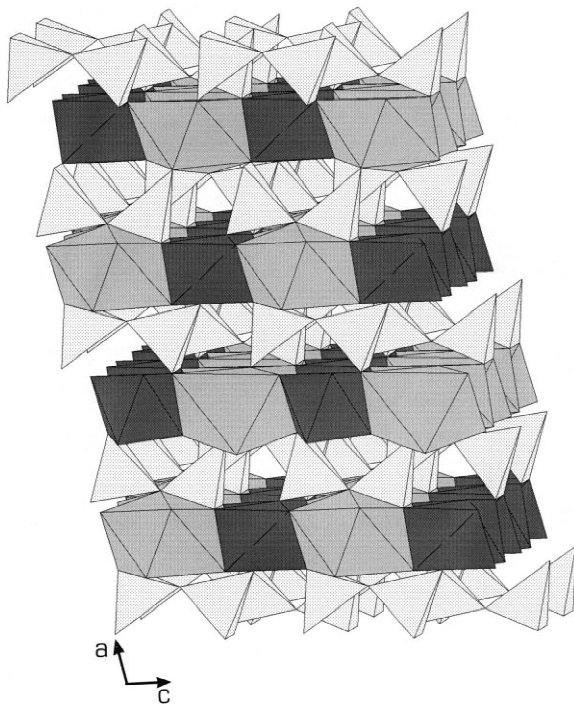


Fig. 3. Complete view of the $\text{DyFeGe}_2\text{O}_7$ structure.

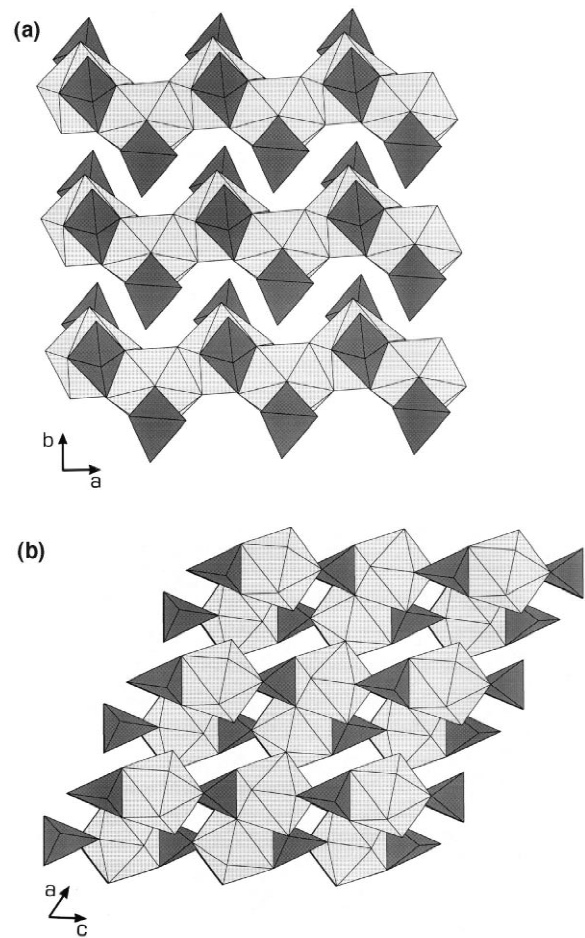


Fig. 4. Projections of the $\text{I-FeRGe}_2\text{O}_7$ ($\text{R}=\text{La–Gd}$) structure showing the RO_7 chains.

the Y-compound, a careful observation of the data reveals the presence of two different anomalies in the thermal variation of χ . Apart from the peaks at 24, 17, 8 and 5 K for $\text{R}=\text{Dy}$, Ho , Er and Yb , respectively, and the broad maximum at 20 K for $\text{R}=\text{Tb}$ [4], there is another anomaly at higher temperature. It consists of a second smaller peak around 40 K in all cases, more visible in the derivative of the product χT with respect to T . For the Y-compound only one maximum at 40 K is observed. Fig. 5 and Fig. 6 correspond to $\text{R}=\text{Dy}$ and Er respectively.

Thus, a qualitative difference can be observed when these χ vs T plots are compared with the reported curves for the compounds with $\text{R}=\text{La}$, Pr , Nd and Gd [3]. As it was shown clear maxima appeared at very low temperatures, 3.1, 2.2, and 5.9 K for the three last compounds respectively, confirming the existence of antiferromagnetic ordering in the rare earth sublattice.

In the low temperature neutron diffraction studies for $\text{FeTbGe}_2\text{O}_7$ [4] and now for $\text{FeDyGe}_2\text{O}_7$, the existence of three dimensional antiferromagnetic ordering has been confirmed for both Fe^{3+} and R^{3+} (Tb , Dy) sublattices, at $T_N=42$ K and 41 K, respectively. The propagation vector of the magnetic structure is in both cases $[0,0,0]$. At lowest

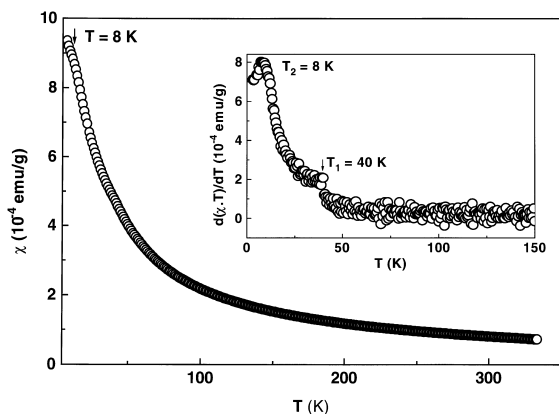


Fig. 5. Magnetic susceptibility for $\text{ErFeGe}_2\text{O}_7$. For sake of clarity in the general plot all experimental points do not appear. The two anomalies are detailed in the inset.

temperature Fe^{3+} and R^{3+} magnetic moments lie ferromagnetically coupled in the ac planes, forming relatively small angles with the c axis. The coupling between parallel ac planes is antiferromagnetic in the b direction. It is clear that the onset of the magnetic order coincides with the higher temperature maximum, T_1 , in each susceptibility

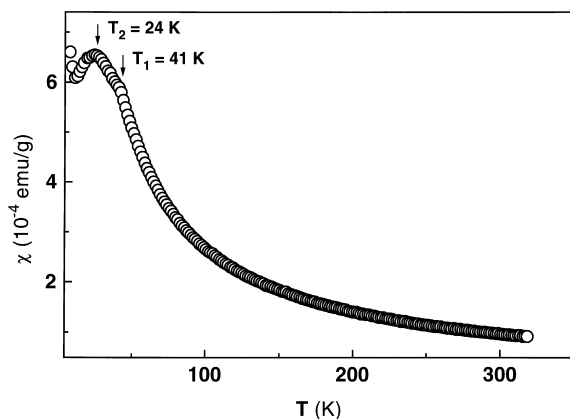


Fig. 6. Thermal variation of the magnetic susceptibility for $\text{DyFeGe}_2\text{O}_7$.

curve. The other maximum in $\chi(T)$, T_2 , at 20 or 24 K, corresponds to the polarization of the R^{3+} (Tb, Dy) magnetic moments under the local effective field from ordered Fe^{3+} and to crystal field effects on R^{3+} ground state manifolds. The peaks at $T_2=17, 8$ and 5 K for $\text{R}=\text{Ho, Er}$ and Yb respectively can also be attributed to the same polarization and crystal field effects.

The study of the magnetic structures for all remaining I- and II- FeRGe_2O_7 germanates are currently in progress [7,8].

Acknowledgements

The authors acknowledge the financial support of the CICYT of Spain, under project PB34-0031 and the ILL of Grenoble for making all facilities available.

References

- [1] A.A. Kaminskii, B.V. Mill, A.V. Butashin, E.L. Belokoneva, K. Kurbanov, *Phys. Stat. Sol. (a)* 103 (1987) 575.
- [2] B.V. Mill, S.A. Kazei, S.I. Reiman, S.A. Tamazyan, F.D. Khamdamov, L.Yu. Bykova, *Vestn. Mosk. Gos. Univ. Fiz. Astron.* 28 (1987) 95.
- [3] L. Bucio, C. Cascales, J.A. Alonso, I. Rasines, *J. Phys.: Condens. Matter* 8 (1996) 2641.
- [4] C. Cascales, L. Bucio, E. Gutierrez Puebla, I. Rasines, M.T. Fernández, *Phys. Rev. B.* 57 (1998) 5240.
- [5] Z.A. Kazei, I.A. Kuyanov, R.Z. Levitin, A.S. Marrkosyan, B.V. Mill, S.I. Reiman, V.V. Snegirev, S.A. Tamazyan, *Sov. Phys. Solid State* 31 (1989) 31.
- [6] E.A. Boudreaux, L.N. Mulay, *Theory and Applications of Molecular Paramagnetism*. New York, Wiley, pp. 494–495.
- [7] C. Cascales, L. Bucio, E. Gutierrez Puebla, I. Rasines, M.T. Fernández, 1997 Institut Laue Langevin Experimental Report 5-31-880.
- [8] C. Cascales, E. Gutierrez Puebla, A. Monge, I. Rasines, B. Lebech, 1997 Annual Progress Report of the Condensed Matter Physics and Chemistry Department, Risø National Laboratory, Denmark.